Analysis of the Fully Developed Chute Flow of Granular Materials

Hojin Ahn
Assoc. Mem. ASME

Christopher E. Brennen
Mem. ASME.

Rolf H. Sabersky
Mem. ASME.

California Institute of Technology,
Pasadena, CA 91125

Existing constitutive relations and governing equations have been used to solve for fully developed chute flows of granular materials. In particular, the results of Lun et al. (1984) have been employed and the boundary value problem has been formulated with two parameters (the coefficient of restitution between particles, and the chute inclination), and three boundary values at the chute base wall, namely the values of solid fraction, granular temperature, and mean velocity at the wall. The boundary value problem has been numerically solved by the "shooting method." The results show the significant role played by granular conduction in determining the profiles of granular temperature, solid fraction, and mean velocity in chute flows. These analytical results are also compared with experimental measurements of velocity fluctuation, solid fraction, and mean velocity made by Ahn et al. (1989), and with the computer simulations by Campbell and Brennen (1985b).

1 Introduction

The rapid flow of granular materials is characterized by high deformation rates, and this rapid shearing motion of the flow causes collisions between particles, generating random motion of those particles. The random motions constitute a so-called granular temperature which is a measure of the fluctuation energy in the granular material. Just like the normal thermodynamic temperature, granular temperature is conducted if there is any temperature gradient. That is, fluctuation energy flows from a region of high fluctuation energy to a region of low fluctuation energy by the process of granular conduction.

Though many studies on granular materials draw the analogy with the kinetic theory of gases, there are differences between granular materials and gas molecules. One of the major differences is that the collisions between granular particles are inelastic. This implies that energy dissipation due to inelastic collisions plays an important role in fluctuation energy balance. Therefore, the question of how the flow creates a balance between the generation of fluctuation energy due to shear motions, its dissipation, and granular conducion becomes an important issue to be explored (see Haff (1983, 1986)).

Our knowledge of the rheological behavior of rapidly flowing granular materials has been advanced by several theoretical works. For example, Ogawa et al. (1980), Savage and Jeffrey (1981), Jenkins and Savage (1983), and Lun et al. (1984) have provided constitutive relations which lead to a comprehension of how stresses are associated with solid fraction, shear rate, and granular temperature, and how energy flux is related to granular temperature, solid fraction, and their gradients. These theoretical results have been applied to a simple shear flow. Especially in the work of Lun et al., the ratio of the characteristic mean shear velocity to the granular temperature, and the ratio of shear stress to normal stress, are given as functions of solid fraction and the coefficient of restitution. In application to chute flows, however, theoretical works have faced difficulties due to lack of knowledge of appropriate boundary conditions at the solid wall (for example, see Hui et al. (1984) and Richman and Marciniec (1988)). Furthermore, the nonuniformity of velocity gradient, granular temperature, and solid fraction over the depth of flow complicate the solution of the equations for chute flows.

Computer simulations of Couette flows (for example, Campbell and Brennen (1985a), Walton and Braun (1986a,b), Campbell and Gong (1986), and Campbell (1989)) have added considerably to our knowledge of the rheology of granular material flows. For example, anisotropy of the granular temperature has been found in most computer simulations while most theoretical works assume the temperature to be isotropic. Relatively little work has been done on the computer simulation of gravity flows. Campbell and Brennen (1985b) simulated chute flows with two-dimensional disks, presenting profiles of velocity, solid fraction, and granular temperature over the depth of flow. Walton et al. (1988) have used three-dimensional spheres to simulate gravity flow of particles through arrays of cylindrical horizontal rods and down inclined chutes. Both have employed periodic boundaries which imply steady, fully developed flow.

On the other hand, progress in experimental methods for granular materials has been very limited, being hindered by obvious difficulties involved in making point measurements of velocity, solid fraction, and granular temperature in the interior of granular flows. For example, the granular temperature, in spite of its importance, had not been experimentally measured until Ahn et al. (1988) used fiber-optic displacement probes to measure one component of the granular temperature. The present state of the experimental information on granular flows consists of a number of Couette flow studies (e.g., Savage

Contributed by the Applied Mechanics Division of THE AMERICAN SOCIETY OF MECHANICAL ENGINEERS for publication in the JOURNAL OF APPLIED MECHANICS.

Discussion on this paper should be addressed to the Technical Editor, Prof. Leon M. Keer, The Technological Institute, Northwestern University, Evanston, IL 60208, and will be accepted until two months after final publication of the paper itself in the JOURNAL OF APPLIED MECHANICS. Manuscript received by the ASME Applied Mechanics Division, Apr. 17, 1989; final revision, Nov. 29, 1990.

and McKeown (1983), Savage and Sayed (1984), Hanes and Inman (1985), Craig et al. (1986)) and several studies of flows down inclined chutes (e.g., Bailard (1978), Augenstein and Hogg (1978), Savage (1979), Sayed and Savage (1983), and Ahn et al. (1988, 1989)). The understandable initial objective of some of the Couette flow experiments, such as those of Savage and McKeown, was to produce a simple shear flow with uniform velocity gradient, uniform solid fraction, and hopefully, uniform granular temperature. To this end the surfaces of the solid walls were roughened to create a no-slip condition at the wall though practical engineering applications usually involve smooth walls.

Only recently has the numerical analysis of the flow of granular materials been attempted, partly because the constitutive relations have been unclear and partly because the boundary conditions remain still uncertain. For rapid granular flow, Hui et al. (1984) developed boundary conditions which were derived from the nature of individual grain-wall collisions. Johnson and Jackson (1987) proposed constitutive relations in which frictional and collisional-translational mechanisms are combined for stress transmission. Furthermore, they developed boundary conditions at the wall which relate friction force and slip velocity at the wall with the large-scale roughness of the surface and relate the wall-particle coefficient of restitution and fluctuation energy flux at the wall. Both relations were described in terms of local density and granular temperature. Using these boundary conditions, Johnson and Jackson (1988) attempted to solve numerically the chute flow of granular materials.

Clearly, the limitations involved in an analytical approach to granular material flows lie in the postulated constitutive relations and boundary conditions, and in the assumption that a continuum approach has validity. Therefore, without thorough understanding of constitutive relations and boundary conditions, the analytical results will be of limited value. Furthermore, the continuum assumption implies that the analysis will become of dubious validity when the depth of the flow becomes less than several particle diameters.

2 Analysis of Chute Flows

2.1 The Governing Equations and the Constitutive Equations. In the present analysis of fully developed chute flow, the constitutive equations of Lun et al. (1984) for granular materials are used along with the basic equations of motions. The continuity equation, the momentum equations, and the translational fluctuation energy equation are as follows:

$$\frac{d\rho}{dt} = -\rho \nabla \cdot \mathbf{u} \tag{1}$$

$$\rho \frac{d\mathbf{u}}{dt} = \rho \mathbf{b} - \nabla \cdot \mathbf{P} \tag{2}$$

$$\frac{3}{2}\rho \frac{dT}{dt} = -\mathbf{P}:\nabla \mathbf{u} - \nabla \cdot \mathbf{q} - \gamma. \tag{3}$$

In these equations, $\rho = \rho_p \nu$ represents the bulk density, where ρ_p is the particle density and ν is the solid fraction. The bulk velocity and the body force per unit mass are represented by $\mathbf{u}$ and $\mathbf{b}$, respectively, and $\mathbf{P}$ is the stress tensor. The granular temperature, T, is defined by $(1/3)(\langle u'^2\rangle + \langle v'^2\rangle + \langle w'^2\rangle)$ where u', v', and w' are the three velocity fluctuation components. Finally, $\mathbf{q}$ is the flux of fluctuation energy, and γ is the rate of the dissipation of fluctuation energy per unit volume. In the translational fluctuation energy equation, the term $-\mathbf{P}:\nabla \mathbf{u}$ indicates the work done to the system by the stresses, and the so-called conduction term, $-\nabla \cdot \mathbf{q}$, represents the conduction of the fluctuation energy within the system.

The recent studies of the rheological behavior of rapidly flowing granular materials have provided explicit constitutive expressions most of which have been derived using methodologies from the kinetic theory of gases. Most of them, however, are not applicable over the entire range of solid fraction. For example, the expressions of Jenkins and Savage (1983) fail at the boundary of the free surface of the chute flow. Only the results presented by Lun et al. (1984) seem to be satisfactory for application to chute flows. Following Lun et al., the total stress tensor is written as

$$\mathbf{P} = \left\{ \rho_p g_1(\nu, e_p) T - \rho_p d \frac{8\sqrt{\pi}}{3} \eta \nu^2 g_0 T^{1/2} \nabla \cdot \mathbf{u} \right\} \times \mathbf{I} - 2\rho_p d g_2(\nu, e_p) T^{1/2} \mathbf{S}, \tag{4}$$

where $\mathbf{I}$ is the identity matrix and $\mathbf{S}$ is given as $\mathbf{S} = (1/2)(u_{i,j} + u_{j,i}) - 1/3 u_{k,k}\delta_{ij}$. The particle diameter is d, and $\eta = (1 + e_p)/2$ where e_p is the coefficient of restitution for collisions between particles. The flux vector of fluctuation energy is

$$\mathbf{q} = -\rho_p d (g_3(\nu, e_p) T^{1/2} \nabla T + g_4(\nu, e_p) T^{3/2} \nabla \nu), \tag{5}$$

and the rate of dissipation per unit volume is

$$\gamma = \frac{\rho_p}{d} g_5(\nu, e_p) T^{3/2}. \tag{6}$$

Here, $g_1(\nu,e_p)$, $g_2(\nu,e_p)$, $g_3(\nu,e_p)$, $g_4(\nu,e_p)$, and $g_5(\nu,e_p)$ are the functions of ν and e_p as follows:

$$g_1(\nu,e_p) = \nu + 4\eta\nu^2 g_0,$$

$$g_2(\nu,e_p) = \frac{5\sqrt{\pi}}{96}\left(\frac{1}{\eta(2-\eta)}\frac{1}{g_0} + \frac{8}{5}\frac{3\eta-1}{2-\eta}\nu + \frac{64}{25}\eta\left(\frac{3\eta-2}{2-\eta} + \frac{12}{\pi}\right)\nu^2 g_0\right),$$

$$g_3(\nu,e_p) = \frac{25\sqrt{\pi}}{16\eta(41-33\eta)}\left(\frac{1}{g_0} + \frac{12}{5}\eta\{1+\eta(4\eta-3)\}\nu + \frac{16}{25}\eta^2\left\{9\eta(4\eta-3) + \frac{4}{\pi}(41-33\eta)\right\}\nu^2 g_0\right),$$

$$g_4(\nu,e_p) = \frac{15\sqrt{\pi}}{4}\frac{(2\eta-1)(\eta-1)}{41-33\eta}\left(\frac{1}{\nu g_0} + \frac{12}{5}\eta\right)\frac{d}{d\nu}(\nu^2 g_0),$$

$$g_5(\nu,e_p) = \frac{48}{\sqrt{\pi}}\eta(1-\eta)\nu^2 g_0.$$

And g_0, the radial distribution function, is chosen as suggested by Lun and Savage (1986), as follows:

$$g_0 = \left(1 - \frac{\nu}{\nu^*}\right)^{-2.5\nu^*},$$

where ν^* is the maximum shearable solid fraction for spherical particles; a value of $\nu^* = 0.62$ is used in this analysis. It should be noted that g_1, g_2, g_3, and g_5 are positive quantities for all ν and e_p while g_4 is always negative. Furthermore, g_1 and g_5 vanish as $\nu \to 0$ while g_0, g_2, g_3, g_4, and all the derivatives of g_0, g_1, g_2, g_3, g_4, with respect to ν, do not vanish as $\nu \to 0$.

2.2 The Formulation of the Boundary Value Problem. We shall now apply these governing equations by Lun et al. (1984) to two-dimensional fully developed flow down an inclined plane. In such a flow the derivatives parallel to the plane are zero and the continuity Eq. (1) is automatically satisfied. The momentum Eqs. (2) in the flow direction (x-direction) and in the direction normal to the chute base (y-direction) become

$$\frac{\partial P_{yy}}{\partial y} = -\rho_p \nu g \cos\theta, \tag{7}$$

$$\frac{\partial P_{yx}}{\partial y} = \rho_p \nu g \sin\theta, \tag{8}$$

where θ is the angle of the chute inclination, and g is the gravitational acceleration. Note that for the fully developed chute flow, $-P_{yx}/P_{yy}=\tan\theta$. The energy equation simplifies to

$$0=-P_{yx}\frac{\partial u}{\partial y}-\frac{\partial q_y}{\partial y}-\gamma. \tag{9}$$

The constitutive Eqs. (4) and (5) also simplify. Since $\nabla\cdot\mathbf{u}=0$, the normal and shear stresses become

$$P_{yy}=\rho_p g_1 T, \tag{10}$$

$$P_{yx}=-\rho_p d g_2\frac{\partial u}{\partial y}T^{1/2}, \tag{11}$$

and the y-component of fluctuation energy flux is given as

$$q_y=-\rho_p d\left(g_3 T^{1/2}\frac{\partial T}{\partial y}+g_4 T^{3/2}\frac{\partial \nu}{\partial y}\right). \tag{12}$$

Here the temperature gradient term has no known physical significance. For the sake of comparison, we retain all the terms of Lun et al.

Equations (7)–(9) with (6) and (10)–(12), after nondimensionalization, can be written in the following form:

$$\frac{\partial \nu}{\partial y^*}=-\frac{1}{g_1' T^*}\left(\nu+g_1\frac{\partial T^*}{\partial y^*}\right), \tag{13}$$

$$\begin{aligned}\frac{\partial^2 T^*}{\partial y^{*2}}=\frac{1}{g_1'^2(g_1g_4-g_1'g_3)}\Bigg[&T^* g_1'^3\left\{\frac{g_1^2}{g_2}\tan^2\theta-g_5\right\}+\frac{1}{T^*}\left(\frac{\partial T^*}{\partial y^*}\right)^2\\&\times\left\{\frac{1}{2}g_1'^3 g_3-g_1 g_1'^2 g_3'+\frac{1}{2}g_1 g_1'^2 g_4+g_1^2 g_1' g_4'-g_1^2 g_1'' g_4\right\}\\&+\frac{1}{T^*}\frac{\partial T^*}{\partial y^*}\left\{g_1 g_1' g_4+\left(2g_1 g_1' g_4'-2g_1 g_1'' g_4-g_1'^2 g_3+\frac{1}{2}g_1'^2 g_4\right)\nu\right\}\\&+\frac{1}{T^*}\{g_1' g_4\nu+(g_1' g_4'-g_1'' g_4)\nu^2\}\Bigg],\end{aligned} \tag{14}$$

$$\frac{\partial u^*}{\partial y^*}=\frac{g_1}{g_2}T^{*1/2}\tan\theta. \tag{15}$$

Here the dimensionless spatial coordinate y^*, granular temperature T^*, and mean velocity u^* are defined by

$$y^*=\frac{y}{d},$$

$$T^*=\frac{T}{gd\cos\theta},$$

$$u^*=\frac{u}{\sqrt{gd\cos\theta}}.$$

And in g_1', g_3', g_4', and g_1'', the dashes denote differentiation with respect to ν. These differential equations are nonlinear, and must be solved simultaneously. Equations (13) and (14) can be solved for ν and T^*; u^* follows from Eq. (15). It is important to note that ν and T^* have solutions independent of u^*.

The above system of differential Eqs. (13)–(15) requires boundary conditions both at the wall of the chute base and at the free surface. At the free surface, the stresses and the energy flux, q_y, must vanish. It is clear that all the conditions are satisfied if and only if $\partial T^*/\partial y^*$ vanishes at the free surface. In Eq. (13), when this gradient of the granular temperature tends to zero at the free surface, the gradient of solid fraction is always negative, and thus the solid fraction vanishes in an approximately exponential manner. Since the solid fraction vanishes at the free surface, the gradient of the solid fraction tends to zero. Therefore, the energy flux vanishes because both gradients of granular temperature and solid fraction vanish at the free surface. Note that the gradient of mean velocity also vanishes, since the solid fraction tends to zero at the free surface. Therefore, all the stresses and their derivatives vanish as ν goes to zero, satisfying the momentum equations at the free surface. The energy equation is also satisfied since all three terms in Eq. (9) vanish independently at the free surface.

It transpires that $T=0$ also satisfies all the boundary conditions at the free surface. However, if $T=0$, $\partial q_y/\partial y$ should be zero from the energy Eq. (9). The condition of $\partial q_y/\partial y=0$ at the free surface with $T=0$ yields $\partial T/\partial y=0$ at the free surface. (This can be shown by differentiating Eq. (12) with respect to y.) Therefore, the condition $\partial T/\partial y=0$ is sufficient and necessary to satisfy all the boundary conditions at the free surface.

Hence, the boundary value problem is formulated as follows: The differential Eqs. (13), (14), and (15), are to be solved with three boundary values at the wall (ν, T^*, and u^* at $y^*=0$) and one boundary condition at the free surface ($\partial T^*/\partial y^*=0$). A "shooting method" has been chosen to solve this boundary value problem. That is, for given ν, T^*, and u^* at the wall, a guess is made for the value of $\partial T^*/\partial y^*$ at $y^*=0$. With these four values, the above differential equations are integrated from $y^*=0$ to $y^*=\infty$. If $\partial T^*/\partial y^*$ at $y^*=\infty$ is not zero after integration, another $\partial T^*/\partial y^*$ at $y^*=0$ is tried. This iterative procedure is continued until $\partial T^*/\partial y^*$ at $y^*=\infty$ becomes zero. In practice, as the equations are integrated from 0 to ∞, a finite y_s^* is found at which $\partial T^*/\partial y^*$ is sufficiently small to say that y_s^* is the location of the free surface. Iterations were done until the ratio of the temperature gradient at the free surface to that at the wall became about 10^{-6}, and the differential equations were, for most of cases, integrated up to $y^*=10\sim100$. A fourth-order Runge-Kutta method was employed, and no convergence problems were encountered.

It is noteworthy that the location of the free surface is automatically determined in the present analysis. In other literature, there have been efforts to locate the free surface using various techniques. For example, Johnson and Jackson (1988) have attempted a numerical analysis similar to the present one. In their analysis, the spatial coordinate Y was normalized by h, the depth of flow. Since h is not well defined because often ν vanishes slowly, it was necessary to define a small layer adjacent to the free surface. The location of this layer was then defined as h, and a boundary value problem was solved between $Y=0$ and $Y=h$. Later, the results near $Y=h$ were matched to asymptotic low density solutions in the neighborhood of the free surface. The asymptotic solutions were obtained by demanding that the solid fraction and the derivatives of velocity and granular temperature vanish as $Y\to\infty$.

3 Results of Analysis and Comparisons

3.1 Results of Analysis. As described earlier, the flow properties, ν, T^*, and u^*, were obtained as functions of y^*—the distance from the chute base normalized by the particle diameter. Each result was specified by the two parameters, e_p and $\tan\theta$, and three boundary values at the wall, ν_w, T_w^*, and u_w^*. The results for $\sqrt{T^*}$ and u^* were normalized by $\sqrt{T_w^*}$ and u_w^*, respectively.

Though two parameters and three boundary values created numerous variations, the results could be classified into two distinct types and a transitional type according to the form of the granular temperature profile. The first type is illustrated by the solution shown in Fig. 1 for which $e_p=0.95$, $\tan\theta=0.4$, $T^*=2$, $\nu_w=0.2$, and $u^*=10$. Note that granular temperature increases with distance from the wall. The profile of solid fraction exhibits a monotonic decrease from the wall to the free surface, and it is clear that solid fraction vanishes at the free surface. The profile of mean velocity appears to be roughly parabolic. Near the wall the profile is fairly linear, and the velocity gradient tends to zero at the free surface. The physical location of the free surface, h, is ill-defined in view of the solid fraction profile. One might reach different conclusions about

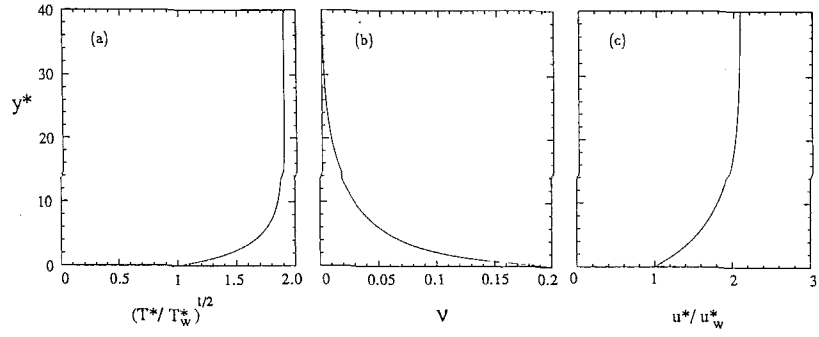

Fig. 1(*a*) Nondimensionalized square root of granular temperature, $(T^*/T_w^*)^{1/2}$, (*b*) solid fraction, ν, and (*c*) nondimensionalized mean velocity, u^*/u_w^*, against nondimensionalized distance from the chute base, y^*. Parameters: $e_p = 0.95$ and $\tan\theta = 0.4$. Boundary values at the wall: $T_w^* = 2$, $\nu_w = 0.2$, and $u_w^* = 10$.

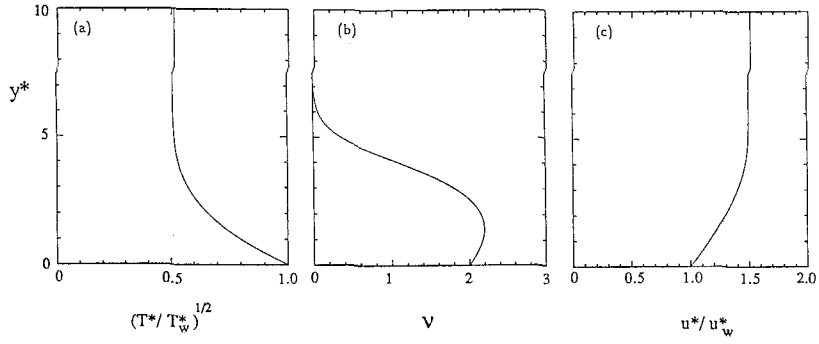

Fig. 2(*a*) Nondimensionalized square root of granular temperature, $(T^*/T_w^*)^{1/2}$, (*b*) solid fraction, ν, and (*c*) nondimensionalized mean velocity, u^*/u_w^*, against nondimensionalized distance from the chute base, y^*. Parameters: $e_p = 0.6$ and $\tan\theta = 0.4$. Boundary values at the wall: $T_w^* = 2$, $\nu_w = 0.2$, and $u_w^* = 10$.

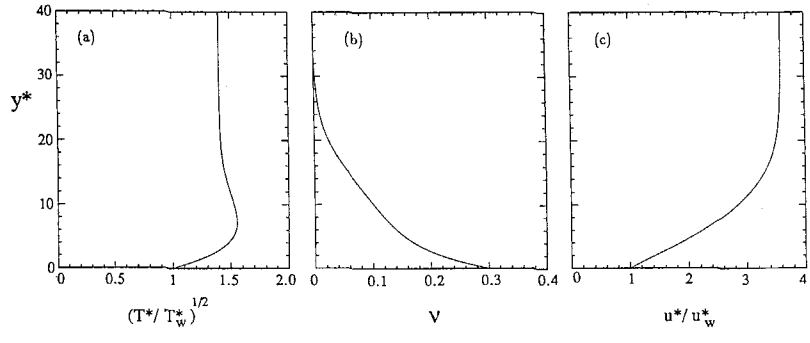

Fig. 3(*a*) Nondimensionalized square root of granular temperature, $(T^*/T_w^*)^{1/2}$, (*b*) solid fraction, ν, and (*c*) nondimensionalized mean velocity, u^*/u_w^*, against nondimensionalized distance from the chute base, y^*. Parameters: $e_p = 0.9$ and $\tan\theta = 0.4$. Boundary values at the wall: $T_w^* = 2$, $\nu_w = 0.3$, and $u_w^* = 10$.

the value of h, depending on whether the granular temperature or the velocity profile is being examined.

Obvious differences in the profile of the granular temperature occur for the second type illustrated in Fig. 2 for which $e_p = 0.6$ and the other values remain unchanged. First of all, the temperature gradient is now negative. The variation of the magnitude of the temperature with distance from the chute based is substantial. The different choice of the value of the coefficient of restitution also results in a particular type of solid fraction profile, where the maximum solid fraction is achieved in the center of the flow and lower densities occur both at the wall and at the free surface. In this case, the free surface is more clearly defined.

Finally, a transitional type, which contains features of both the first and second types, is illustrated in Fig. 3. Note that $e_p = 0.8$ and $\nu_w = 0.3$ while the other parameter and boundary values are not changed. The granular temperature first increases with distance from the wall boundary, then decreases at larger distances from the wall, and then becomes uniform near the free surface. The profile of solid fraction is similar to that of the first type.

The question of when each of these types of the granular temperature profiles occurs will be discussed later. In this presentation, the first, second, and last types will be referred to as Type I, Type II, and Type III, respectively.

The effect of the variation of the parameter $\tan\theta$ is investigated in Fig. 4. The results show that higher gradients of granular temperature and velocity arise from a higher angle of chute inclination, and the depth of flow also increases. This is consistent with a physical understanding of the chute flow.

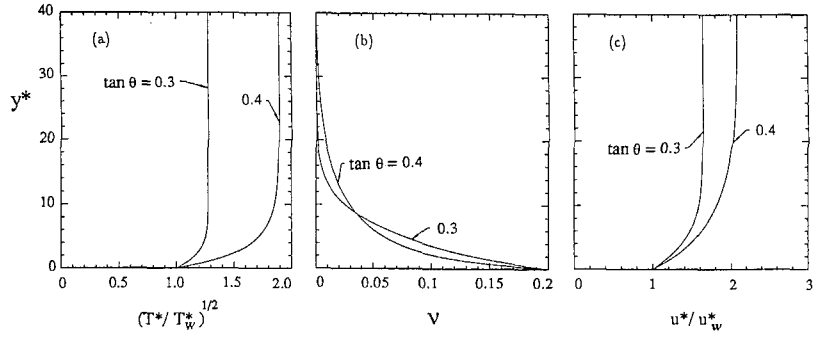

Fig. 4 The effect of the variation of the chute inclination angle. (*a*) Nondimensionalized square root of granular temperature, $(T^*/T_w^*)^{1/2}$, (*b*) solid fraction, ν, and (*c*) nondimensionalized mean velocity, u^*/u_w^*, against nondimensionalized distance from the chute base, y^*. Parameters: $e_p = 0.95$, $\tan\theta = 0.3$, and 0.4. Boundary values at the wall: $T_w^* = 2$, $\nu_w = 0.2$, and $u_w^* = 10$.

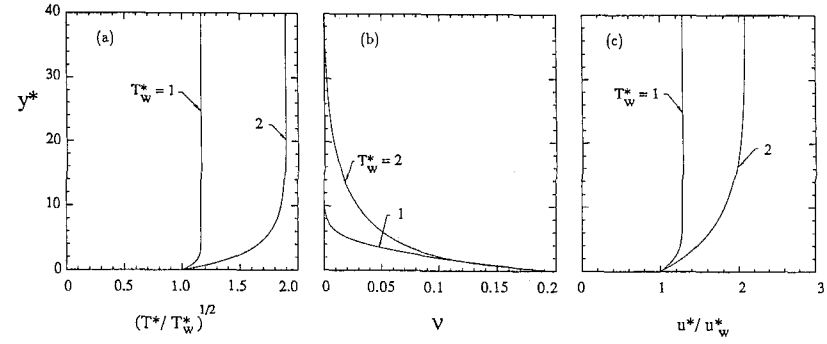

Fig. 5 The effect of the variation of granular temperature at the wall. (*a*) Nondimensionalized square root of granular temperature, $(T^*/T_w^*)^{1/2}$, (*b*) solid fraction, ν, and (*c*) nondimensionalized mean velocity, u^*/u_w^*, against nondimensionalized distance from the chute base, y^*. Parameters: $e_p = 0.95$ and $\tan\theta = 0.4$. Boundary values at the wall: $T_w^* = 1$ and 2, $\nu_w = 0.2$, and $u_w^* = 10$.

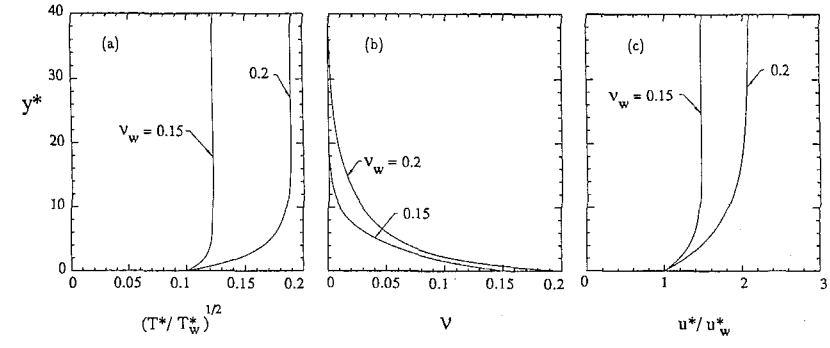

Fig. 6 The effect of the variation of solid fraction at the wall. (*a*) Nondimensionalized square root of granular temperature, $(T^*/T_w^*)^{1/2}$, (*b*) solid fraction, ν, and (*c*) nondimensionalized mean velocity, u^*/u_w^*, against nondimensionalized distance from the chute base, y^*. Parameters: $e_p = 0.95$ and $\tan\theta = 0.4$. Boundary values at the wall: $T_w^* = 2$, $\nu_w = 0.15$ and 0.2, and $u_w^* = 10$.

That is, for a higher inclination angle, particles move faster and collide with greater impact, resulting in the increase of granular temperature and velocity gradient. The increase of the overall granular temperature causes dilatation near the wall which is accompanied by an increase in the depth of flow. As a result, the solid fraction for the higher chute inclination is lower near the wall, but higher at a distance from the wall.

The effect of the variation of boundary values at the wall is examined in Figs. 5 and 6. Comparison shows that a larger value of granular temperature at the wall results in an increase in the granular temperature gradient and thus the overall granular temperature as shown in Fig. 5. As a consequence, (see Eq. (15)), the gradient of mean velocity also increases. The increase of granular temperature is also accompanied by an increase in the depth of flow. These results are consistent with the experimental observations of Ahn et al. (1989). On the surface where higher temperature is created, higher gradients of temperature and velocity are observed, and the depth of flow is increased.

The effect of the variation of solid fraction at the wall is examined in Fig. 6. When a larger solid fraction is prescribed at the wall, the granular temperature, the depth of flow, and

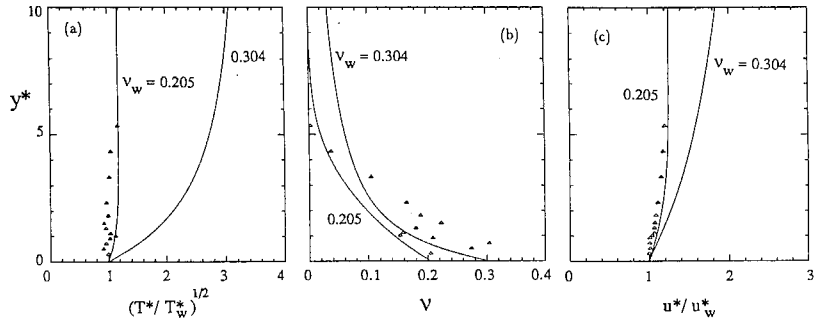

Fig. 7 Comparison with the experimental data of Ahn et al. (1989). The smooth aluminum surface used for the chute base and $d = 1.26$ mm Δ, data from the experiment. Solid line results of the present analysis. (*a*) Nondimensionalized square root of granular temperature, $(T^*/T^*_w)^{1/2}$, (*b*) solid fraction, ν, and (*c*) nondimensionalized mean velocity, u^*/u^*_w, against nondimensionalized distance from the chute base, y^*. Parameters: $e_p = 0.95$ and $\tan\theta = 0.418$. Boundary values at the wall: $T^*_w = 0.935$, $\nu_w = 0.205$ and 0.304, and $u^*_w = 11.3$.

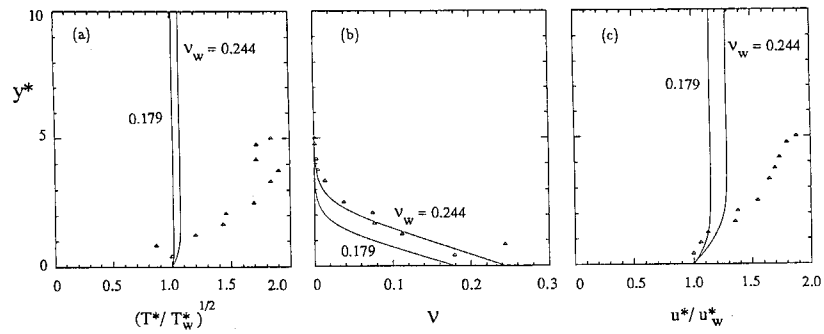

Fig. 8 Comparison with the experimental data of Ahn et al. (1989). The rubber-coated surface used for the chute base and $d = 3.04$ mm Δ, data from the experiment. Solid line results of the present analysis. (*a*) Nondimensionalized square root of granular temperature, $(T^*/T^*_w)^{1/2}$, (*b*) solid fraction, ν, and (*c*) nondimensionalized mean velocity, u^*/u^*_w, against nondimensionalized distance from the chute base, y^*. Parameters: $e_p = 0.95$ and $\tan\theta = 0.418$. Boundary values at the wall: $T^*_w = 0.440$, $\nu_w = 0.179$ and 0.244, and $u^*_w = 4.39$.

the mean velocity all increase significantly. These results agree with the experimental observations. In order to have a high solid fraction at a given chute inclination, the mass flow rate needs to be large and this implies a deeper flow.

3.2 Comparison with Experimental Results. Few experimental data are available for comparison with these analytical results. In particular, there are almost no measurements of granular temperature. Furthermore, the wall boundary conditions are not sufficiently well understood to allow us to estimate the values of T^*, ν, and u^* at the wall. The experiments of Ahn et al. (1989) represent an attempt to acquire the necessary data. In measurements through the sidewalls, the profiles of one component of granular temperature, mean velocity, and linear concentration were obtained. For comparison with the present results, granular temperature and solid fraction are obtained from one component of granular temperature, $\langle u'^2 \rangle$, and linear concentration, ν_{1D}, by taking $T = \langle u'^2 \rangle$ and $\nu = \pi\nu^3_{1D}/6$. Furthermore, the value of $e_p = 0.95$ is appropriate for the glass beads used in the experiments (see Lun and Savage (1986)) and this value of e_p is employed in all the results presented.

In a strict sense the solid fraction goes to zero at the wall since the particles are spherical. As a result, the appropriate wall solid fraction to be used in the corresponding continuum model is rather unclear. Therefore, two candidate choices are employed in the comparisons which follow. One is the solid fraction which was obtained at the measurement location closest to the wall. The other is the maximum solid fraction which was usually obtained at between a half and one-particle diameter distance from the wall.

Experimental data for 1.26-mm diameter glass beads flowing down a chute with a smooth aluminum surface are compared with the present analysis in Fig. 7. The chute inclination angle θ was 22.7 deg, and the boundary values at the wall, $T^*_w = 0.935$ and $u^*_w = 11.3$ are taken from the experiments. Two wall solid fractions are used as described above, namely, 0.205 and 0.304. The profile of granular temperature from the experiments shows a general increase of temperature with distance from the wall. This increasing feature is predicted by the present analysis. With $\nu_w = 0.205$, the magnitude of granular temperature is also well predicted. Moreover, the monotonic decrease of solid fraction with distance from the wall is consistent with the experiments. Near the wall, the result for the case of $\nu_w = 0.304$ shows better agreement with the experiments, but at the free surface, the present analytical result deviates from the experiments. For $\nu_w = 0.205$, the depth of flow of the analysis is consistent with that of the experiments while there is slight discrepancy near the wall. In addition, good agreement is observed between the profiles of mean velocity for the case of $\nu_w = 0.205$.

For the second comparison, experimental data with a rubber-coated chute base are presented in Fig. 8. This rubber-coated surface created quite different boundary conditions. Compared to a smooth aluminum surface, the depth of flow was high, mean velocity was usually low, and both the gradients of mean velocity and granular temperature were high. In the

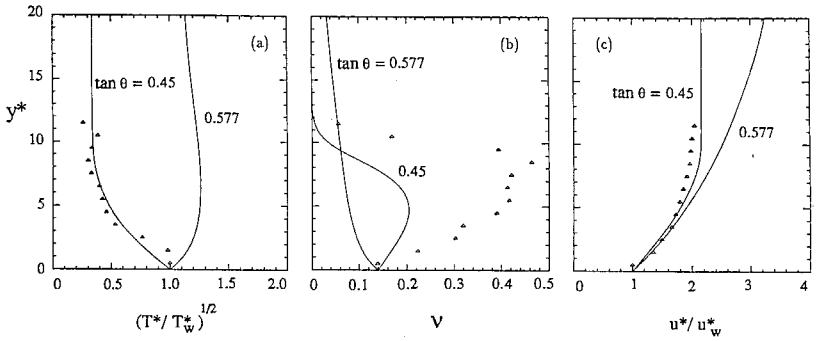

Fig. 9 Comparison with the computer simulations by Campbell and Brennen (1985b). Δ, data from the computer simulations. Type A simulation with $\theta = 30$ deg, $e_p = 0.6$, and $e_w = 0.8$. Solid line, results of the present analysis. Parameters: $e_p = 0.6$, and $\tan\theta = 0.577$ and 0.45. Boundary values at the wall: $T_w^* = 7.00$, $\nu_w = 0.140$, and $u_w^* = 14.0$. (*a*) Nondimensionalized square root of granular temperature, $(T^*/T_w^*)^{1/2}$, (*b*) solid fraction, ν, and (*c*) nondimensionalized mean velocity, u^*/u_w^*, against nondimensionalized distance from the chute base, y^*.

experiments, the 3.04-mm glass beads were used, and the chute inclination angle was 22.7 deg. Boundary values at the wall, $T_w^* = 0.44$ and $u_w^* = 4.388$ are taken from the experiments, and $\nu_w = 0.179$ and $\nu_w = 0.244$ are chosen as alternative solid fractions at the wall. Considerable discrepancy is observed between the profiles of granular temperature. The present analysis yields almost uniform granular temperature while the experimental data display significant granular conduction from the free surface to the wall. On the other hand, a remarkable agreement is found in the profiles of solid fraction, especially in the case of $\nu_w = 0.244$. The depth of flow as well as the general shape of solid fraction profile is well predicted in the present analysis. In the profiles of mean velocity, a deviation of the analysis from the experimental data is found. The discrepancies found in the profiles of granular temperature and mean velocity could be a result of the experimental flow not being fully developed. One might surmise that this flow would obtain a higher granular temperature as it becomes fully developed. If a large value of T_w^* were used in the present analysis, considerable increases of granular temperature and mean velocity would result (as shown in Fig. 5).

3.3 Comparison with Computer Simulation. Comparison of the present analysis can also be made with the computer simulations of Campbell and Brennen (1985b). The results of Campbell and Brennen for $\theta = 30$ deg or $\tan\theta = 0.557$, $e_p = 0.6$, and $e_w = 0.8$ and their Type A boundary condition are presented in Fig. 9. The results, with two-dimensional disks, were converted into three-dimensional values by taking $\nu_{3D} = 4\nu_{2D}^{3/2}/3\sqrt{\pi}$ and $T = (1/2)(\langle u'^2\rangle + \langle v'^2\rangle)$. The boundary values were $T_w^* = 7$, $u_w^* = 14$, and $\nu_w = 0.14$. The results of the present analysis with these parameters and boundary values are shown in Fig. 9. When $\tan\theta = 0.577$ is used as a parameter in the analysis, a fundamental difference is found. The results of Campbell and Brennen are of Type II, while the present analysis yields a Type III flow. However, when $\tan\theta = 0.45$ is used for the analysis, comparison shows excellent agreement between the analysis and the computer simulation. Both profiles of granular temperature have negative gradients, and their magnitudes are also in good agreement. The profiles of solid fraction are qualitatively similar, and the depth of flow is also well predicted. A discrepancy in the magnitude of solid fraction may arise from the fact that the computer simulations were done with two-dimensional disks. In the case of $\tan\theta = 0.45$, the mean velocity profiles also show good agreement between the computer simulation and the present analysis.

In short, good agreement is achieved in the case of $\tan\theta = 0.45$, which is slightly different from the value of the computer simulation. This may imply that the present analysis confirms the possibility of the existence of Type II flow but does not accurately predict when that type of flow takes place.

The results of Campbell and Brennen's computer simulations at the small chute angle of $\theta = 20$ deg could not be reproduced by the present analysis. The analysis yielded a Type II temperature profile, while the computer simulations produced a type of plug flow. That is, the minimum granular temperature was achieved in the center of the flow and higher temperature occurred both at the wall and at the free surface. The solid fraction profile of the analysis was similar to Type I while the computer simulation result had the profile of Type II.

Comparisons of the present analysis with experiments and computer simulations lead to the following conclusions: The experimental data are similar to Type I flow in which a positive temperature gradient and monotonically decreasing solid fraction are observed. The present analysis also produces the results of Type I as long as the boundary values are properly chosen. The general profiles of flow properties are well predicted, though some discrepancies in their magnitudes are observed. On the other hand, the computer simulations have Type II flows for sufficiently high chute inclinations. The granular temperature decreases with distance from the wall, and the solid fraction increases near the wall and decreases with further distance from the wall. These results can also be produced by the present analysis when a slight change in the parameter $\tan\theta$ is made.

The fundamental difference between the experimental results and the computer simulations is the value of the coefficient of restitution ($e_p = 0.95$ for the experiments and $e_p = 0.6$ for the computer simulations). The different values of e_p result in Type I flow for the experiments and Type II flow for the computer simulations. This will be discussed further in the next section.

4 The Nature of Granular Conduction

For fully developed chute flows, the translational fluctuation energy Eq. (9) may be written as follows:

$$W + Q - \gamma = 0$$

where W is the rate of the work done by stresses to the system per unit volume, Q is the rate of conduction of the fluctuation energy within the system, and γ is the dissipation rate per unit volume. For a simple shear flow, the conduction term disappears from the energy equation. But for chute flows, the role of the conduction term, or its magnitude compared to the other two terms, has been unclear. Haff (1986) emphasized the importance of grain inelasticity during a discussion of the

conduction and damping length scales. In this section, the fundamental nature of the conduction term will be discussed.

For fully developed chute flow, the ratio of shear stress to normal stress is a constant, given by $\tan\theta$. Using the constitutive equations for the stresses presented in Eqs. (10) and (11), the ratio of the characteristic velocity gradient to the granular temperature, often known as S or R in the literature, is given as follows:

$$S=\frac{d\dfrac{du}{dy}}{T^{1/2}}=\frac{\dfrac{du^*}{dy^*}}{T^{*1/2}}=\frac{g_1}{g_2}\tan\theta.$$

Recall that g_1 and g_2 are functions only of e_p and ν. Therefore, S is a function not only of e_p and ν but also of $\tan\theta$, while for Couette flows it is a function only of e_p and ν. Note S vanishes at the free surface since g_1 tends to zero as $\nu\to 0$.

The explicit form of S makes it possible to evaluate the work done by shear stress, and thus all the terms in the fluctuation energy equation are given as follows:

$$W^*=\frac{g_1^2}{g_2}T^{*3/2}\tan^2\theta,$$

$$\gamma=g_5T^{*3/2}$$

$$Q^*=\gamma^*-W^*,$$

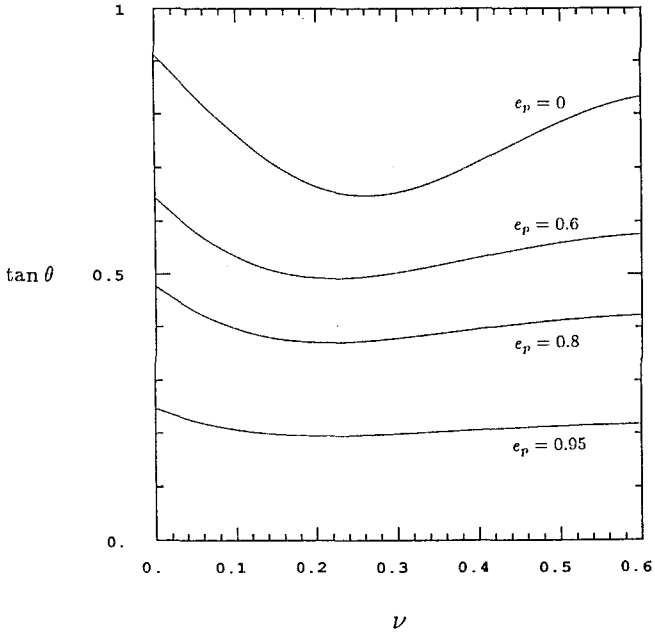

Fig. 10 Zeros of the granular conduction term for various e_p.

where W^*, γ^*, and Q^* are shear work term, dissipation term, and granular conduction term nondimensionalized by $\rho_p(gd\cos\theta)^{3/2}/d$. Furthermore, it is recalled that

$$Q^*=-\frac{\partial q^*}{\partial y^*},$$

where q^*, the fluctuation energy flux nondimensionalized by $\rho_p(gd\cos\theta)^{3/2}$, is given as

$$q^*=-\left(g_3T^{*1/2}\frac{\partial T^*}{\partial y^*}+g_4T^{*3/2}\frac{\partial \nu}{\partial y^*}\right).$$

It can be noted from the constitutive equations that γ^* is quite sensitive to the value of e_p while W^* is less sensitive, and that γ^* vanishes as e_p approaches 1. Therefore, for large e_p (e.g. 0.95), W^* is larger than γ^*, and this results in a negative value of Q^*. The opposite is true for small e_p such as 0.6. For a positive Q^*, the gradient of q^* is negative, and a positive gradient of q^* is achieved for negative Q^*. But the boundary condition at the free surface requires that $q^*\to 0$ as $y^*\to\infty$. Consequently, for a fixed ν, a negative value of q^* is obtained for all y^* in the case of a positive gradient of q^*, and a positive value of q^* in the case of a negative gradient of q^*. In other words, for a sufficiently large e_p, a negative energy flux, q^*, is achieved along with a negative granular conduction term Q^*. And for a sufficiently small e_p, a positive Q^* results in a positive energy flux.

As ν varies over the depth of the flow, however, the above argument may need modification. The effects of ν and $\tan\theta$ on the conduction term can be examined along with the effect of e_p as follows: The zero of Q^* is found by examining the following equation for Q^*

$$Q^*=\left(g_5-\frac{g_1^2}{g^2}\tan^2\theta\right)T^{*3/2}=0.$$

This is solved as shown in Fig. 10. Each curve represents zeros of Q^* for a given e_p. If $\tan\theta$ is greater than the value on the curve for a given ν, negative values of Q^* are obtained, and if $\tan\theta$ is smaller, then $Q^*>0$. For example, for $\tan\theta=0.4$, negative values of Q^* result for all ν in the case of $e_p=0.95$, but positive values result in the case of $e_p=0.6$.

The effects of e_p, ν, and $\tan\theta$ on the conduction term were examined in detail for solutions of Type I, Type II, and Type III flows. The energy flux, q^*, and the conduction term, Q^*, are plotted in Fig. 11(*a*), (*b*), and (*c*) with the same parameters and boundary values as given in Figs. 1, 2, and 3, respectively. As expected from the results of Fig. 10 in the case of $e_p=0.95$ and $\tan\theta=0.4$, negative Q^* is achieved in Fig. 11(*a*) and thus negative q^*. But for $e_p=0.6$ and $\tan\theta=0.4$ in Fig. 11(*b*), positive Q^* and q^* emerge, which are in accordance with the results of Fig. 10. When q^* is negative at the wall boundary it means that the wall absorbs the fluctuation energy. For this

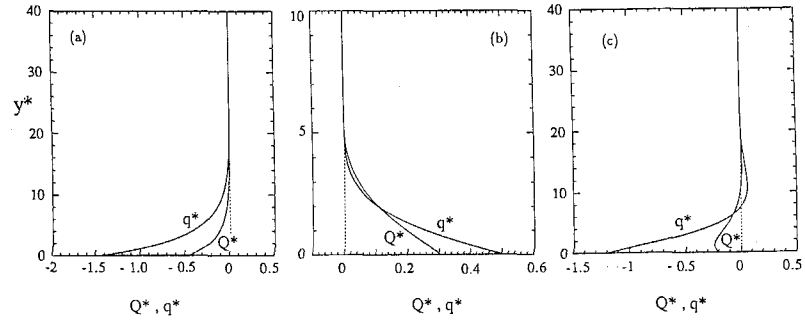

Fig. 11 Nondimensionalized granular conduction, Q^*, and fluctuation energy flux, q^*, against nondimensionalized distance from the chute base, y^*. Parameters and boundary values at the wall; (*a*) as in Fig. 1, (*b*) as in Fig. 2, and (*c*) as in Fig. 3.

case, the granular temperature is expected to be low near the wall while high temperature is exhibited at the free surface, and thus the fluctuation energy is conducted from the free surface to the wall. The generation of fluctuation energy through shear motion feeds fluctuation energy into the bulk, where it is partly absorbed at the wall boundary and partly dissipated away. On the other hand, positive fluctuation energy flux at the wall implies that the wall should supply energy to the flow. Unless energy is provided to granular materials through the wall (for example, by vibrating the chute base), there can be no such positive fluctuation energy flux and therefore no such flow. (Note that changes to granular material flows wrought by vibration are well known in industrial practice.) In the experiments of Ahn et al. (1989) when the angle of the chute inclination was less than about 12 deg, there was no flow unless the chute was agitated. This is consistent with the results of Fig. 10 in which the zero of Q^* for $e_p = 0.95$ is achieved at $\tan\theta \simeq 0.22$.

With this idea in mind, it is interesting to study a hypothetical experiment in which there is no shear motion but granular materials are allowed to have granular temperature which might be supplied by wall vibration. Then fluctuation energy will be conducted from the wall and should all be dissipated inside the bulk. Now examine such a state using the present analysis. The mean velocity and its gradient are zero, and $\tan\theta = 0$. From Fig. 10 it is expected that the conduction term will be positive for all values of the coefficient of restitution. The solutions are illustrated in Fig. 12 in which $e_p = 0.9$ and 0.95, $\tan\theta = 0$, $\nu_w = 0.2$, and $T_w^* = 5$. As expected, the solutions are of Type II because of a positive conduction term. Temperature decreases with distance from the wall, and solid fraction increases near the wall but decreases with further distance from the wall. Comparison between the results for different values of e_p show

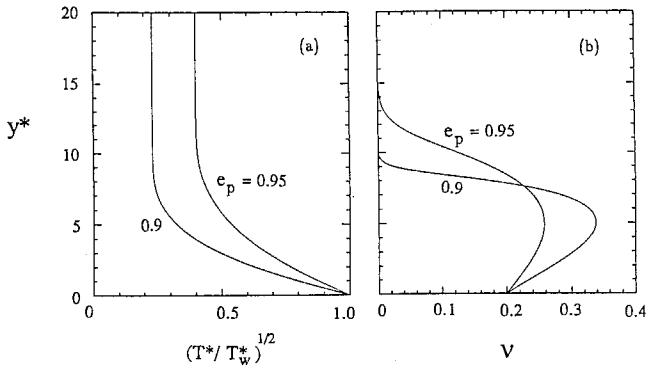

Fig. 12 The study of the case in which no shear motion and mean velocity exist. (*a*) Nondimensionalized square root of granular temperature, $(T^*/T_w^*)^{1/2}$, and (*b*) solid fraction, ν, against nondimensionalized distance from the chute base, y^*. Parameters: $e_p = 0.9$ and 0.95, and $\tan\theta = 0$. Boundary values at the wall: $T_w^* = 5$ $\nu_w = 0.2$.

as expected that for low e_p, the fluctuation energy dissipates faster than for high e_p. Therefore, the case of the lower e_p results in a lower temperature at the free surface.

At this point, it is necessary to study how solid fraction varies with granular temperature. Physically, it is clear that it is difficult for particles to stay close in the presence of high temperature. Therefore, when the temperature is high, the solid fraction is low. The variation of solid fraction with granular temperature can be explained in more detail by using Eq. (13):

$$\frac{\partial \nu}{\partial y^*} = -\frac{1}{g_1' T^*}\left(\nu + g_1 \frac{\partial T^*}{\partial y^*}\right).$$

When the temperature gradient is negative, the solid fraction gradient can be positive since both g_1 and g_1' are always positive. Therefore, when the temperature decreases significantly with distance from the wall, the solid fraction increases near the wall as shown in Figs. 2 and 12. Furthermore, when the temperature is lower, the magnitude of the solid fraction gradient is higher. Hence, the solid fraction for $e_p = 0.9$ increases more than for $e_p = 0.95$ as shown in Fig. 12. Equation (13) also explains the variation of solid fraction near the free surface. Near the free surface g_1' tends to 1, g_1 is the same order as ν, and the temperature gradient is negligible. Therefore, ν decreases approximately as e^{-y^*/T^*}. When the temperature is low at the free surface, a rapid decrease of solid fraction occurs. Therefore, the free surface is clearly defined as shown in Fig. 2. On the other hand, when the temperature is high near the free surface, the solid fraction decreases slowly with distance, resulting in the case of Fig. 1.

Figure 11(*c*) is an interesting case for which q^* and Q^* start with negative values but become positive and tend to zero as the free surface is approached. The boundary values at the wall ($\nu = 0.3$) and the two parameters ($e_p = 0.8$ and $\tan\theta = 0.4$) give a negative value of Q^* from Fig. 10. As ν decreases from the wall to the free surface, a positive Q^* is to be obtained from Fig. 10. This particular profile of energy flux over the depth gives rise to the particular shape of temperature profile in Fig. 3. Note from Fig. 11(*c*) that a local maximum of q^* is achieved when $Q^* = 0$.

The fundamental question of the magnitude of the conduction term in the chute flow is answered in Fig. 13 where the ratio of the conduction term to the dissipation term is plotted against y^*. Figures 13(*a*), (*b*), and (*c*) are the results from cases of Figs. 1, 2, and 3, respectively. In none of Figs. 13(*a*) and (*b*) is the conduction term insignificant relative to the dissipation term. In an transitional case such as Fig. 13(*c*), the conduction term is relatively smaller than the dissipation term. In fact, the ratio of the conduction term to the dissipation term is given as follows:

$$\frac{Q^*}{\gamma^*} = 1 - \frac{g_1^2}{g_2 g_5}\tan^2\theta.$$

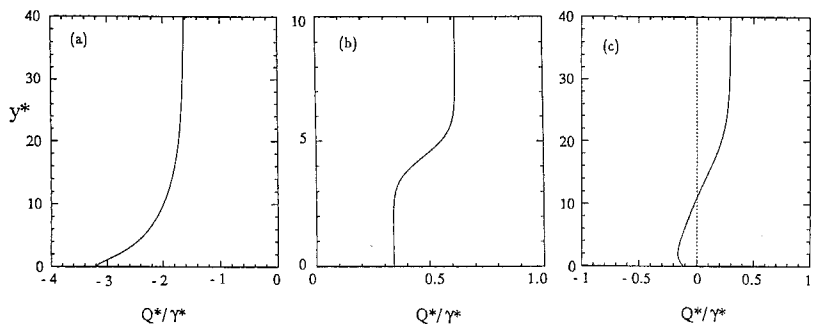

Fig. 13 The ratio of granular conduction to dissipation, Q^*/γ^*, against nondimensional distance from the chute base, y^*. Parameters and boundary values at the wall: (*a*) as in Fig. 1, (*b*) as in Fig. 2, and (*c*) as in Fig. 3.

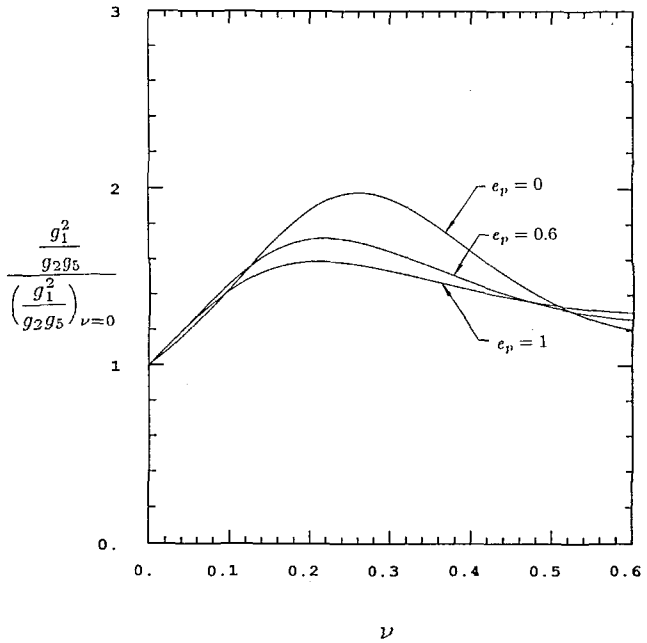

Fig. 14 The function g_1^2/g_2g_5 for various e_p, normalized by g_1^2/g_2g_5 at $\nu=0$

In Fig. 14, g_1^2/g_2g_5, normalized by the value at $\nu=0$, is plotted as a function of ν and e_p. Note that g_1^2/g_2g_5 at $\nu=0$ is given as follows:

$$\left(\frac{g_1^2}{g_2g_5}\right)_{\nu=0} = \frac{2}{5}\left(\frac{3-e_p}{1-e_p}\right).$$

Therefore, Q^*/γ^* varies from 1(when $\theta=0$) to $-\infty$ (when $e_p=1$), and conduction is always important. In general, the magnitude of the ratio is large for large e_p and small for small e_p. When negative conduction exists, a higher chute inclination yields a larger value for the ratio. That is, for a higher chute inclination, the conduction term plays a more important role relative to the dissipation term than for a lower chute inclination. When the conduction is positive, the opposite is true.

Since $W^*/\gamma^* = 1 - Q^*/\gamma^*$, the shear work term is small compared to the dissipation term when the conduction term is positive. When the conduction term is negative, W^*/γ^* is relatively large. (Note the comparison between Figs. 13(*a*) and (*b*)). When W^*/γ^* is small (such as the case of Fig. 13(*b*)) granular temperature is low, because fluctuation energy is slowly generated by the shear work. Furthermore, the flow dissipates well because of a low coefficient of restitution. As a result, the high density at the center of the flow is not dilated (see Fig. 2).

5 Conclusion

The governing equations and the constitutive relations presented by Lun et al. (1984) have been used in the present analysis of fully developed chute flow. The boundary value problem has been formulated with two parameters (e_p and $\tan\theta$). Three boundary values at the wall (ν_w, T_w, and u_w) are required for the solution. It is found that all the boundary conditions at the free surface are satisfied if and only if the gradient of temperature vanishes at the free surface. This boundary value problem has been numerically solved by a "shooting method."

The solutions fall into two categories: Only the two parameters (e_p and $\tan\theta$) determine which type of flow will occur, and three boundary values at the wall play no role in determining the type of flow. The first type has a granular temperature which increases from the wall boundary to the free surface. The solid fraction monotonically decreases with distance from the chute base, and the free surface is not well defined. The second type exhibits high temperature near the chute base, and a rapid decrease of the temperature as the free surface is approached. In this type the solid fraction is low at both boundaries but high in the center of the flow, and the free surface is rather clearly defined. A transitional type is also found which exhibits features of both the first and second types of flow; the temperature increases near the wall but decreases thereafter. The solid fraction has a profile similar to the first type.

These profiles are closely connected to the role of the granular conduction term in the fluctuation energy equation. The conduction term, which depends on e_p, $\tan\theta$, and ν, determines the energy flux, and thus the gradients of granular temperature and solid fraction, causing different profiles to occur. The conduction term often appears to be significant in magnitude compared to the dissipation term.

The effect of the variations of the parameter and wall boundary values is also studied. As the chute inclination angle increases, granular temperature, mean velocity, and the depth of flow increase. A higher granular temperature at the wall also causes an overall increase in temperature, mean velocity, and flow depth. An increase in the solid fraction at the wall also yields the same result.

Comparisons with experiments and computer simulations have been made. The experiments of Ahn et al. (1989) correspond to Type I flows. The experimental data show that with distance from the chute base the solid fraction decreases monotonically, and granular temperature increases indicating granular conduction from the free surface to the wall. The results of the present analysis are consistent with those data. The general profiles of flow properties are well predicted, though some discrepancies in their magnitudes are observed. On the other hand, the computer simulations by Campbell and Brennen (1985b) correspond to Type II flows. Granular conduction from the wall to the free surface is observed, and the solid fraction is low at both boundaries but high in the bulk. Good agreement between the present analysis and the computer simulations is found when a slightly different value of the parameter $\tan\theta$ is used as an input. The decrease of granular temperature with distance from the wall is well predicted, and the profile of solid fraction is similar to that of the computer simulations. Some discrepancies may be due to the fact that the computer simulations were conducted with two-dimensional disks.

The different types of flow occurring in the experiments and the computer simulations are the results of the different values of the coefficient of restitution appropriate to those circumstances. A high value of e_p, such as the value of about 0.95 in the experiments, causes the granular temperature to be conducted from the free surface to the wall; and a low value of e_p, such as the value of 0.6 used in the computer simulations, results in granular conduction in the opposite direction.

References

Ahn, H., Brennen, C. E., and Sabersky, R. H., 1988, "Experiments on Chute Flows of Granular Materials," *Micromechanics of Granular Materials*, M. Satake and J. T. Jenkins, eds., Elsevier, Amsterdam, pp. 339–348.

Ahn, H., Brennen, C. E., and Sabersky, R. H., 1989, "Measurements of Velocity, Velocity Fluctuation, Density, and Stresses in Chute Flows of Granular Materials," ASME JOURNAL OF APPLIED MECHANICS, to be published.

Augenstein, D. A., and Hogg, R., 1978, "An Experimental Study of the Flow of Dry Powders on Inclined Surfaces," *Powder Technology*, Vol. 19, pp. 205–215.

Bailard, J., 1978, "An Experimental Study of Granular-Fluid Flow," Ph.D. Thesis, University of California, San Diego.

Campbell, C. S., 1989, "The Stress Tensor for Simple Shear Flows of a Granular Material," *J. Fluid Mech.*, to be published.

Campbell, C. S., and Brennen, C. E., 1985a, "Computer Simulation of Granular Shear Flows," *J. Fluid Mech.*, Vol. 151, pp. 167–188.

Campbell, C. S., and Brennen, C. E., 1985b, "Chute Flows of Granular

Material: Some Computer Simulations," ASME JOURNAL OF APPLIED MECHANICS, Vol. 52, pp. 172–178.

Campbell, C. S., and Gong, A., 1986, "The Stress Tensor in a Two-Dimensional Granular Shear Flow," *J. Fluid Mech.*, Vol. 164, pp. 107–125.

Craig, K., Buckholz, R. H., and Domoto, G., 1986, "An Experimental Study of the Rapid Flow of Dry Cohesionless Metal Powders," ASME JOURNAL OF APPLIED MECHANICS, Vol. 53, pp. 935–942.

Haff, P. K., 1983, "Grain Flow as a Fluid Mechanical Phenomenon," *J. Fluid Mech.*, Vol. 134, pp. 401–430.

Haff, P. K., 1986, "A Physical Picture of Kinetic Granular Fluids," *J. Rheology*, Vol. 30, No. 5, pp. 931–948.

Hanes, D. M., and Inman, D. L., 1985, "Observations of Rapidly Flowing Granular-Fluid Flow," *J. Fluid Mech.*, Vol. 150, pp. 357–380.

Hui, K., Haff, P. K., Ungar, J. E., and Jackson, R., 1984, "Boundary Conditions for High-Shear Grain Flows," *J. Fluid Mech.*, Vol. 145, pp. 223–233.

Jenkins, J. T., and Savage, S. B., 1983, "A Theory for the Rapid Flow of Identical, Smooth, Nearly Elastic Particles," *J. Fluid Mech.*, Vol. 130, pp. 187–202.

Johnson, P. C., and Jackson, R., 1987, "Frictional-Collisional Constitutive Relations for Granular Materials, With Application to Plane Shearing," *J. Fluid Mech.*, Vol. 176, pp. 67–93.

Johnson, P. C., and Jackson, R., 1988, "Frictional-Collisional Equations of Motion for Particulate Flows and Their Application to Chutes," submitted to *J. Fluid Mech.*

Lun, C. K. K., and Savage, S. B., 1986, "The Effects of an Impact Velocity Dependent Coefficient of Restitution on Stresses Developed by Sheared Granular Materials," *Acta Mechanica*, Vol. 63, pp. 15–44.

Lun, C. K. K., Savage, S. B., Jeffrey, D. J., and Chepurniy, N., 1984, "Kinetic Theories for Granular Flow: Inelastic Particles in Couette Flow and Slightly Inelastic Particles in a General Flowfield," *J. Fluid Mech.*, Vol. 140, pp. 223–256.

Ogawa, S., Umemura, A., and Oshima, N., 1980, "On the Equations of Fully Fluidized Granular Materials," *J. App. Math. Phys. (ZAMP)*, Vol. 31, pp. 483–493.

Richman, M. W., and Marciniec, R. P., 1988, "Gravity-Driven Granular Flows of Smooth, Inelastic Spheres Down Bumpy Inclines," submitted to ASME JOURNAL OF APPLIED MECHANICS.

Savage, S. B., 1979, "Gravity Flow of Cohesionless Granular Materials in Chutes and Channels," *J. Fluid Mech.*, Vol. 92, pp. 53–96.

Savage, S. B., and Jeffrey, D. J., 1981, "The Stress Tensor in a Granular Flow at High Shear Rates," *J. Fluid Mech.*, Vol. 110, pp. 255–272.

Savage, S. B., and McKeown, S., 1983, "Shear Stress Developed During Rapid Shear of Dense Concentrations of Large Spherical Particles Between Concentric Cylinders," *J. Fluid Mech.*, Vol. 127, pp. 453–472.

Savage, S. B., and Sayed, M., 1984, "Stresses Developed by Dry Cohesionless Granular Materials in an Annular Shear Cell," *J. Fluid Mech.*, Vol. 142, pp. 391–430.

Sayed, M., and Savage, S. B., 1983, "Rapid Gravity Flow of Cohesionless Granular Materials Down Inclined Chutes," *J. Appl. Math. Phys.*, Vol. 34, pp. 84–100.

Walton, O. R., and Braun, R. L., 1986a, "Viscosity, Granular-Temperature, and Stress Calculations for Shearing Assemblies of Inelastic, Frictional Disks," *J. of Rheology*, Vol. 30, No. 5, pp. 949–980.

Walton, O. R., and Braun, R. L., 1986b, "Stress Calculations for Assemblies of Inelastic Spheres in Uniform Shear," *Acta Mechanica*, Vol. 63, pp. 73–86.

Walton, O. R., Braun, R. L., Mallon, R. G., and Cervelli, D. M., 1988, "Particle-Dynamics Calculations of Gravity Flow of Inelastic, Frictional Spheres," *Micromechanics of Granular Materials*, M. Satake and J. T. Jenkins, eds., Elsevier, Amsterdam, pp. 153–162.